Optical Fiber Technology 17 (2011) 201–209

Contents lists available at ScienceDirect

Optical Fiber Technology

www.elsevier.com/locate/yofte

Analysis of multimode POF gratings in stress and strain sensing applications

Yanhua Luo [a,b,*], Binbin Yan [b,c], Mo Li [b], Xiaolei Zhang [b], Wenxuan Wu [a], Qijin Zhang [a], Gang-Ding Peng [b]

[a] CAS Key Laboratory of Soft Matter Chemistry, Department of Polymer Science and Engineering, Anhui Key Laboratory of Optoelectronic Science and Technology, University of Science and Technology of China, Hefei, Anhui 230026, China
[b] School of Electrical Engineering and Telecommunications, University of New South Wales, Sydney 2052, Australia
[c] Key Laboratory of Information Photonics and Optical Communications of Ministry of Education, Beijing University of Posts and Telecommunications, Beijing 100876, China

ARTICLE INFO

Article history:
Received 21 August 2010
Revised 29 January 2011
Available online 21 March 2011

Keywords:
Polymer optical fiber
Polymer optical fiber gratings
Multimode POF gratings
Stress sensing
Strain sensing

ABSTRACT

Polymer fiber Bragg gratings (FBGs) are made using the modified sagnac system with a 355 nm pulsed laser from a photosensitive polymer optical fiber (POF) with external and core diameters of 290.6 and 21.0 μm, respectively. Multimodes are reflected based on the reflection spectra of the gratings. The reflectivity spectra are also studied when such multimode polymer FBGs are subjected to axial static stress and strain. The respective effects of stress and strain on the sensor are decoupled and analyzed independently. Experiments and regression show that the effect of stress and the relaxation of stress in multimode FBGs (MM FBGs) in POF during loading and unloading have a more evident non-linear effect than that of strain. These non-linear properties make FBGs attractive for mechanical sensing applications.

1. Introduction

In recent years, polymer optical fibers (POFs) have attracted much research attention because they present unique characteristics, such as flexibility, ease of use and relatively low cost; POFs are also popularly used in coupling because of their large core diameter [1–3]. With the development of POFs, numerous research activities have been carried out in this field, and of these, one area of interest is POF gratings [4–16]. Since its first demonstration in 1999 [13], gratings written in POF have attracted great research interest for their high sensitivity to strain and temperature, wide tuning wavelength range, good biocompatibility, etc. [4,6,14,17–19]. Due to these characteristics, POF gratings are widely used in marine, civil, and aeronautical engineering sectors [17,20,21]. Numerous studies on POF gratings have been conducted, and different kinds of POF gratings have been created including both the single-mode fiber Bragg gratings (SM FBGs) and the multimode FBGs (MM FBGs) [4–16].

SM FBGs in POF are widely used in strain and temperature sensors, humidity detectors, fiber lasers with wide tuning wavelength range, etc. [4,6,14,17–21]; in comparison, applications of MM FBGs in POF are still rare. However, MM FBGs in POF actually posses the merits of both multimode FBGs and POF gratings, including easy coupling with low cost light sources for distributed sensing networks [22–24], efficient relationship between information energy and input energy, noise reduction by fitting >10 narrow peaks instead of 1 broad envelope (correlation of multi-peaks of different height requires an algorithm of image recognition) [25], high sensitivity to strain and temperature, wide tuning wavelength range, good biocompatibility, etc. Therefore, the fabrication of fiber sensor gratings in multimode POFs and applications of MM FBGs in POF are of great interest. Hence, MM FBGs in POF were fabricated in this work; in addition, stress and strain sensing properties of such MM FBGs were investigated systematically. Owing to the viscoelastic character of POF [21], the non-linear stress and strain effect for MM FBGs in POF were also independently discussed and analyzed in detail.

2. Theoretical background

When an axial strain is applied to MM FBGs in POF, the wavelength of the ith reflection mode (λ_{bi}) is shifted by an amount, $\Delta\lambda_{bi}$, due to strain-inducing changes of the periodicity and the effective refractive index. The strain effect could be expressed as [26,27]:

$$\Delta\lambda_{bi} = \lambda_{bi}(1 - p_{eff})\varepsilon_z, \tag{1}$$

where ε_z is the axial strain on the grating, and p_{eff} is the effective strain-optic constant.

For classic elastomers, stress (σ) and strain (ε_z) satisfy the following relationship:

$$\sigma = E \cdot \varepsilon_z, \tag{2}$$

* Corresponding author at: CAS Key Laboratory of Soft Matter Chemistry, Department of Polymer Science and Engineering, Anhui Key Laboratory of Optoelectronic Science and Technology, University of Science and Technology of China, Hefei, Anhui 230026, China. Fax: +86 551 3601704.
E-mail address: yhluo3@mail.ustc.edu.cn (Y. Luo).

1068-5200/$ - see front matter © 2011 Elsevier Inc. All rights reserved.
doi:10.1016/j.yofte.2011.02.005

where E is the Young's modulus. Considering the elasticity of POF alone and neglecting its viscoelasticity, the relationship between stress (σ) and axial strain (ε_z) of POF can also be described using Eq. (2).

The relationship between stress (σ) and the force (F) applied on the fiber is expressed by:

$$\sigma = \frac{F}{A} = \frac{4F}{\pi D^2}, \tag{3}$$

where A is the area of the cross section of the fiber and D is the diameter of the fiber.

If POF is an elastomer, then combining Eqs. (1)–(3) yields:

$$\Delta\lambda_{bi} = \lambda_{bi}\frac{(1-p_{eff})}{E}\sigma, \tag{4}$$

where $\lambda_{bi}\frac{(1-p_{eff})}{E}$ is obtained by linear fitting, which gives an estimated value of E.

However, polymers are viscoelastic materials and, as such, the measured Young's modulus changes when stress is applied. For gradually-loaded stress, strain increases non-linearly with stress loading [28]. When the stress is removed, recovery occurs and strain decreases non-linearly with the stress unloading [21]. Therefore, Eq. (4) is hardly satisfied and results in:

$$\Delta\lambda_{bi} = \sum_{n=1}^{k} K_n\sigma^n, \tag{5}$$

where K_n is the polynomial coefficient fitting, and k is the best fitting polynomial order used. When $k = 1$, $K_1 = \lambda_{bi}\frac{(1-p_{eff})}{E}$ is used to describe the elastomer.

3. Fabrication of MM FBGs in POF

Benzildimethylketal (BDK) containing POF shown in Fig. 1 was made through the Teflon technique. In this method, BDK is activated by a transition in the molecular orbits of the >C=O group followed by α-splitting to produce free radicals irradiated by UV light to induce a change in the refractive index [29,30]. Using the Teflon technique, a hollow stick was made from the copolymer of MMA and butyl acrylate (BA) according to a previously reported procedure [31,32]. At this point, 7 ml MMA was mixed with 0.6986 g BDK, along with 11.6 mg azo-bis-isobutyronitrile as the initiator and 25.2 μL n-butyl mercaptan as the chain-transfer agent. Under 7 atm N_2, the solution filled the hollow stick as a core material, after which thermal polymerization was then carried out. The temperature was increased gradually from 45 to 75 °C within 4 days until solidification. The preform was then heat-drawn into an optical fiber at 120 °C by a taking up spool. POFs with different diameters were made by tuning the drawing velocity and mould diameter. The parameters of the POF sample are listed in Table 1. The fiber and core diameters of POF doped with BDK were 290 and 21 μm, respectively. The cladding refractive index and the refractive index difference between the core and cladding were about 1.4862 and 0.011 (633 nm), respectively.

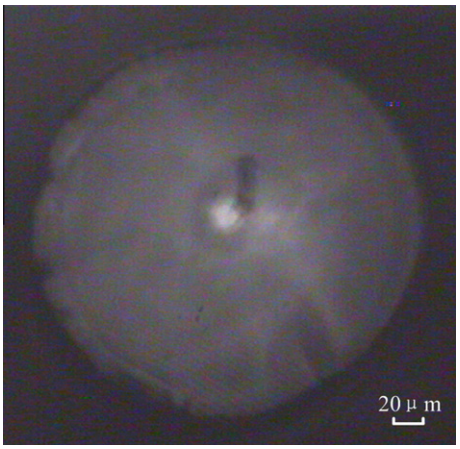

Fig. 1. Cross section of POF doped with benzildimethylketal (BDK).

To fabricate FBGs in POF, the modified sagnac optical ring system was used with a 355 nm frequency-tripled Nd:YAG pulse laser (Fig. 2); this technique also helped overcome the effect of zeroth-order diffraction on the grating writing in optical fibers. A phase mask with a period of 1.0614 μm designed for 248 nm operation was used. The phase mask diffracted the Nd:YAG laser into three main orders:±1 and 0. Two first-order beams were diverted from the zeroth-order diffraction by three prisms that formed interference beams for grating writing, after which the zeroth-order diffraction was isolated and blocked. Polymer fiber was placed on the top of the phase mask (Fig. 2), and three reflective prisms were aligned so that the counter-propagating coherence beams were directed to the fiber to write the grating. In order to monitor grating formation, ASE (Thorlabs ASE-FL7002) was launched into POF through a 3 dB single mode silica fiber coupler. Upon reaching the grating, a portion of the light was reflected while the rest propagated through the grating and down the fiber. An optical spectrum analyzer (Agilent 86140B OSA) was then used to detect the reflection and determine the reflection spectrum of the grating. The grating fabrication conditions are described in Table 1.

Grating formation in 10.6 cm POF doped with BDK was detected by introducing ASE light into the POF through a silica optical fiber coupler. And then an optical spectrum analyzer (Agilent 86140B OSA) monitored the grating formation by detecting its reflection spectrum. The laser beam was not focused and had an effective spot size of 6 mm. The calculated normalized frequency at 1570 nm was ~5.4. This value is larger than the maximum limit (2.405) for the single mode condition; hence, multimodes are expected as shown in Fig. 3. Meanwhile, the reflected modes of the reflection spectra of the polymer FBG at different exposure times are also presented (Fig. 3a).

Given that reflection peak position slightly changed with time (Fig. 3b), this could be attributed to temperature and mechanical drift. The plot of the maximum reflection peak (around 1574.3 nm) intensity and exposure time is shown in Fig. 3b. A noticeable reflection peak appeared after 1 min of exposure, after which the grating continued to grow stronger with further exposure. After 6 min, the maximum reflection spectrum was obtained; this peak was about 1574.3 nm and had a 5.1 dB peak with FWHM of about 0.3 nm. After 8 min, the grating reflection peak began to decrease, indicating onset of the grating decaying process. After 10 min of UV illumination, the irradiation turned OFF. The reflection of FBGs was not high because of the multimode effect and drifting of the writing system; in addition, growth and decay of polymer FBG during UV exposure was observed. These could be attributed to the increase of refractive index change during the

Table 1
Fiber parameters and grating fabrication conditions.

POF specification	Grating formation process
Cladding(MMA-BA 69/31)	355 nm frequency-tripled Nd:YAG pulse laser
Core(MMA-BA62.4:28 + 9.6wt% BDK)	
Index difference between core and cladding, ~0.011	10 Hz, 6 ns pulse width
Fiber optical diameter, ~290 μm	One beam average intensity:153 mW/cm^2
Fiber core diameter, ~21 μm	
Fiber length, 10.6 cm	Grating length, 6 mm